Electronic Supporting Information for

A photochromic-acidochromic HCl fluorescent probe. An unexpected chloride-directed recognition

Arturo Jiménez-Sánchez[a],* and Rosa Santillan[b]

[a] Facultad de Química, Universidad Nacional Autónoma de México, 04510 México D.F., México.

[b] Departamento de Química, Centro de Investigación y de Estudios Avanzados del IPN, CINVESTAV, Apdo., Postal 14-740, México, D. F. 07000, México.

Fax: 55 5616 2010; Tel: 55 5622 3813; E-mail: arturo@cinvestav.mx

To whom correspondence should be addressed: arturo@cinvestav.mx

Synthesis and characterization

4-(Dimethylaminophenyl)allylideneamino-1-aminomethyl-1-cyclohexanol (**S1**). Schiff base derivative **S1** was prepared through the condensation reaction of 4-dimethylamino-*trans*-cinnamaldehyde (1.00 g, 5.7 mmol) and 1-aminomethyl-1-cyclohexanol (0.74 g, 5.7 mmol), stirring for 2 h under reflux of methanol. The solvent and water formed during the reaction were removed with a Dean-Stark trap to yield a solid, which was washed with *n*-hexane/ethyl acetate mixtures (9:1), to give 1.58 g (5.4 mmol, >95% yield) of **S1**. m.p.: 165-167ºC. ^{1}H NMR (DMSO-δ_6, 300 MHz) δ: 7.95 (1H, d, $J = 9.0$ Hz, N_{imine} proton), 7.43 (2H, d, $J = 9.0$ Hz), 6.97 (1H, d, $J = 15.0$ Hz), 6.73 (2H, d, $J = 6.0$ Hz), 3.99 (1H, s) 3.38-3.35 (4H, d) 2.97 (6H, s), 1-7-1.1 (11H, m) ppm. Anal. Calcd. for $C_{18}H_{26}N_2O$: C 75.48, H 9.15, N 9.78; found: C 75.61, H 9.52, N 9.71. HR-ESI-MS: *m*/*z* for $C_{18}H_{26}N_2O$ $[M^+ +H]$: 286.2042; found: 286.2043 (error 0.0521 ppm).

^{1}H NMR spectrum for **S1** in DMSO-δ_6, 300 MHz

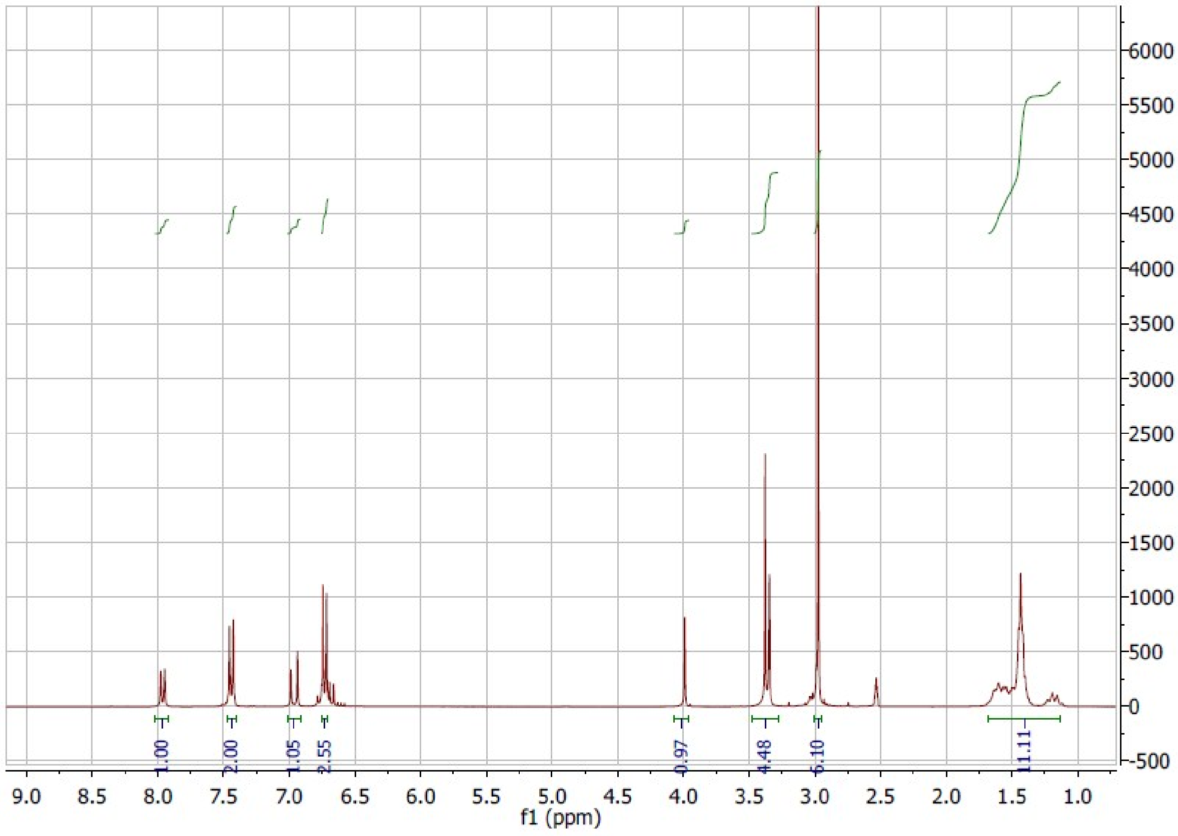

Table S1 Summary of crystal data for **S1** at 293 K

Compound	**S1**
Crystal color	Red
Empirical formula	$C_{18}H_{27}N_2OCl$
Mol wt.	322.88
Crystal System	Monoclinic
Space group	$P2_1$/a
a (Å)	14.388(2)
b (Å)	6.189(3)
c (Å)	20.392(2)
α (°)	90
β (°)	98.158
γ (°)	90
V (Å^3)	1797.48(5)
Z	4
$\rho_{calcd.}$ (g/cm^3)	1.190
Θ Range (°)	27.20
F(000)	696.0
Abs. Coeff. (mm$^-$	0.217
No. of reflections:	
Measured	11102
Unique	3883
Observed	2637
R [I > 2σ(I)]	0.055
Rw (all data)	0.090
Parameters	204
ρ_{min} (e Å^3)	-0.206
ρ_{max} (e Å3)	0.178
GOOF	1.041

Table S1b. *Geometric parameters (Å, º)*

Special details 30 Geometry All e.s.d.'s (except the e.s.d. in the dihedral angle between two l.s. planes) are estimated using the full covariance matrix. The cell e.s.d.'s are taken into account individually in the estimation of e.s.d.'s in distances, angles and torsion angles; correlations between e.s.d.'s in cell parameters are only used when they are defined by crystal symmetry. An approximate (isotropic) treatment of cell e.s.d.'s is used for estimating e.s.d.'s involving l.s. planes.

Fractional atomic coordinates and isotropic or equivalent isotropic displacement parameters (Å^2)

	x	**y**	**z**	**U_{iso}*/U_{eq}**
C1	0.11357 (14)	0.9005 (3)	1.06998 (10)	0.0431 (5)
C2	0.15199 (14)	1.1004 (3)	1.05494 (10)	0.0466 (5)
H2	0.1676	1.2014	1.0885	0.056*
C2A	0.09109 (15)	0.7538 (3)	1.01703 (10)	0.0479 (5)
H2A	0.0649	0.6206	1.0249	0.057*
C3	0.16671 (14)	1.1486 (3)	0.99158 (10)	0.0449 (5)
H3	0.1914	1.2830	0.9831	0.054*
C3A	0.10726 (15)	0.8045 (3)	0.95430 (10)	0.0480 (5)
H3A	0.0920	0.7039	0.9206	0.058*
C4	0.14585 (13)	1.0022 (3)	0.93925 (10)	0.0417 (5)
C5	0.16721 (14)	1.0558 (3)	0.87420 (10)	0.0471 (5)
H5	0.1915	1.1932	0.8693	0.057*

C6	0.15615 (15)	0.9301 (4)	0.81964 (10)	0.0485 (5)
H6	0.1327	0.7907	0.8220	0.058*
C7	0.17974 (14)	1.0074 (3)	0.75882 (10)	0.0475 (5)
H7	0.2054	1.1451	0.7578	0.057*
C8	0.19243 (15)	0.9747 (4)	0.64209 (10)	0.0502 (5)
H8A	0.1846	1.1304	0.6398	0.060*
H8B	0.1497	0.9118	0.6061	0.060*
C9	0.29305 (14)	0.9185 (3)	0.63302 (9)	0.0435 (5)
C10	0.31057 (16)	1.0087 (4)	0.56629 (11)	0.0589 (6)
H10A	0.2631	0.9531	0.5319	0.071*
H10B	0.3043	1.1647	0.5669	0.071*
C11	0.40716 (18)	0.9510 (5)	0.54943 (13)	0.0721 (7)
H11A	0.4124	1.0009	0.5050	0.086*
H11B	0.4548	1.0240	0.5799	0.086*
C12	0.42410 (18)	0.7097 (5)	0.55343 (14)	0.0798 (9)
H12A	0.4880	0.6797	0.5462	0.096*
H12B	0.3821	0.6385	0.5187	0.096*
C13	0.40838 (17)	0.6189 (4)	0.62014 (14)	0.0692 (7)
H13A	0.4552	0.6771	0.6545	0.083*
H13B	0.4155	0.4631	0.6199	0.083*
C14	0.31053 (16)	0.6762 (4)	0.63520 (12)	0.0565 (6)
H14A	0.2640	0.6057	0.6032	0.068*
H14B	0.3032	0.6221	0.6788	0.068*
C15	0.1190 (2)	1.0001 (5)	1.18696 (12)	0.0791 (8)
H15A	0.1040	0.9352	1.2269	0.119*
H15B	0.1844	1.0370	1.1926	0.119*
H15C	0.0820	1.1283	1.1774	0.119*
C15A	0.0576 (2)	0.6438 (4)	1.14711 (12)	0.0682 (7)
H15D	0.0526	0.6367	1.1935	0.102*
H15E	-0.0037	0.6308	1.1218	0.102*
H15F	0.0967	0.5281	1.1357	0.102*
N1	09853 (14)	0.8483 (3)	1.13249 (9)	0.0555 (5)
N2	16764 (12)	0.8975 (3)	0.70494 (9)	0.0483 (4)
O1	34878 (10)	1.0263 (3)	0.68645 (7)	0.0588 (4)
H1	4045	1.0084	0.6836	0.088*
Cl10	0.07460 (4)	0.45625 (10)	0.71228 (3)	0.0680 (2)
H100	0.1427 (16)	0.764 (4)	0.7049 (11)	0.059 (7)*

Geometric parameters (Å,°)

C1—N1	1.362 (3)	C8—N2	1.459 (3)
C1—C2	1.407 (3)	C8—C9	1.526 (3)
C1—C2A	1.412 (3)	C9—O1	1.424 (2)
C2—C3	1.372 (3)	C9—C14	1.520 (3)
C2A—C3A	1.369 (3)	C9—C10	1.525 (3)
C3—C4	1.400 (3)	C10—C11	1.521 (3)
C3A—C4	1.396 (3)	C11—C12	1.513 (4)
C4—C5	1.442 (3)	C12—C13	1.518 (4)
C5—C6	1.348 (3)	C13—C14	1.525 (3)
C6—C7	1.415 (3)	C15—N1	1.452 (3)
C7—N2	1.283 (3)	C15A—N1	1.445 (3)
N1—C1—C2	122.14 (18)	O1—C9—C10	111.40 (18)
N1—C1—C2A	120.92 (18)	C14—C9—C10	109.86 (18)
C2—C1—C2A	116.94 (18)	O1—C9—C8	103.97 (16)
C3—C2—C1	120.98 (18)	C14—C9—C8	112.17 (18)

C3A—C2A—C1	121.09 (19)	C10—C9—C8	107.74 (16)
C2—C3—C4	122.16 (19)	C11—C10—C9	112.82 (19)
C2A—C3A—C4	122.15 (19)	C12—C11—C10	111.4 (2)
C3A—C4—C3	116.67 (18)	C11—C12—C13	111.7 (2)
C3A—C4—C5	123.18 (18)	C12—C13—C14	110.7 (2)
C3—C4—C5	120.11 (18)	C9—C14—C13	112.16 (19)
C6—C5—C4	127.6 (2)	C1—N1—C15A	121.61 (18)
C5—C6—C7	120.9 (2)	C1—N1—C15	121.40 (19)
N2—C7—C6	123.4 (2)	C15A—N1—C15	116.93 (19)
N2—C8—C9	112.73 (16)	C7—N2—C8	123.9 (2)
O1—C9—C14	111.53 (17)		

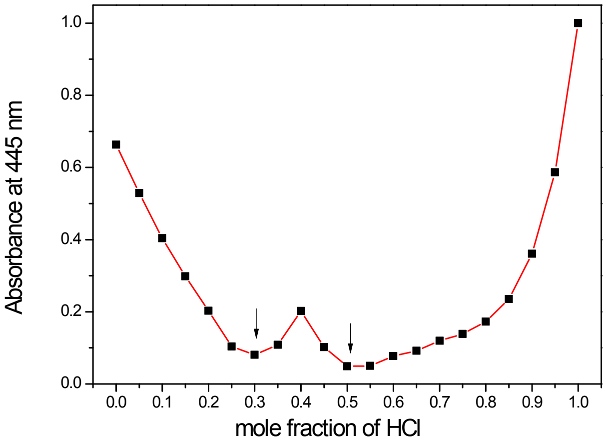

Figure S1. Continuous variation curve (Job's plot) for probe **S1** *vs.* HCl in water evaluated at 445 nm. The final concentration was 10 μM.

Table S2. Solvatochromic analysis for **HCl·S1** crystals

Solvent	*E*	*n*	*Δf*	λ_a *(nm)*	$\bar{\nu}_a$ *(cm^{-1})*	λ_e *(nm)*	$\bar{\nu}_e$ *(cm^{-1})*	$\bar{\nu}_a$–$\bar{\nu}_e$ *(cm^{-1})*
Cyclohexane	2.02	1.4235	0	350	28571	397	25136	3435
Dioxane	2.22	1.4224	0.021	353	28328	411	24325	4004
Toluene	2.38	1.4961	0.013	357	28011	413	24216	3795
Diethyl ether	4.27	1.3526	0.165	351	28491	409	24457	4034
MTBE	4.50	1.3690	0.1161	351	28491	412	24268	4223
Chloroform	4.81	1.4459	0.148	467	21413	515	19416	1997
BAc	5.07	1.3940	0.1163	358	27933	422	23652	4281
EAc	6.081	1.3723	0.201	354	28248	421	23751	4497
THF	7.52	1.4050	0.210	356	28090	419	23873	4216
DCM	8.93	1.4242	0.217	361	27700	426	23468	4233
Octanol	10.30	1.4295	0.225	364	27472	431	23197	4275
***i*-PrOH**	20.18	1.3776	0.277	361	27700	436	22931	4770
Acetone	21.01	1.3588	0.285	354	28248	434	23044	5204
EtOH	24.65	1.3611	0.289	363	27548	442	22626	4922
MeOH	33.00	1.3288	0.308	463	21598	517	19342	2255
ACN	36.64	1.3442	0.305	355	28169	441	22672	5497
DMF	36.70	1.4305	0.274	357	28011	444	22526	5485
EG	41.40	1.4320	0.276	467	21413	524	19083	2331
DMSO	46.68	1.4793	0.263	359	27855	455	21986	5869
Water	80.40	1.3325	0.279	464	21552	527	18975	2577

a: Dielectric constant, (*ε*), refractive index, (*n*);[49] Orientation polarizability, (*Δf*); absorption wavelength, (λ_o); absorption wavenumber, ($\bar{\nu}_a$); emission wavelength, (λ_e); emission wavenumber, ($\bar{\nu}_e$). Solvent notation: MTBE (methyl *t*-butyl ether), THF (tetahydrofuran), DCM (dichloromethane), *i*-PrOH (*iso*-propanol), BAc (butyl acetate), EAc (ethyl acetate), EtOH (ethanol), MeOH (methanol), ACN (acetonitrile), DMF (Dimethylformamide), EG (Ethylene Glycol), DMSO (Dimethyl sulfoxide).

The various contributions to the electronic excitation can be clarified by a Natural Transition Orbital (NTO) analysis,[79] which provides a compact orbital representation of the electronic transition through a single configuration of a hole and electron interaction. Consequently, the photoinduced electron transfer process is not depicted by a simple change in the elementary molecular orbital occupancy, but in a hole – electron distribution. Then, to have a better understanding of the multiresponse mechanism of probe **S1**, the representative transition energy diagram for the HOMO–LUMO orbitals was obtained, Figure S2. In general, the calculated NTO distributions show that the electronic transitions within **S1** are dominated by an ICT character due to the HOMO–LUMO levels for the whole system, assigned to a $\pi \rightarrow \pi^*$ electronic transition. Moreover, the ICT character in [HCl(**S1**)] is not maintained, and a decrease in the transition energy of the HOMO–LUMO vertical excitation arises with the HOMO level located *ca.* 0.46 eV below the HOMO level of **S1**, therefore, the ICT process prohibits the radiative deactivation (fluorescence). The

NTO coefficients (*w*) representing the extent to which the electronic excitation can be written as a single excitation are 0.99, and 1.0 for **S1** and [HCl(**S1**)], respectively.

	Hole	**Particle**
S1 329.1 nm; f = 1.210; 78 – 79; w = 0.99	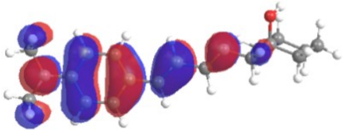	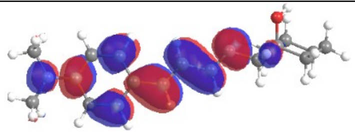
S1-HCl 959.7 nm; f = 0.008; 87 – 88 w = 0.99	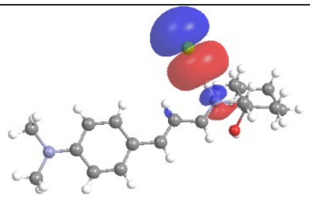	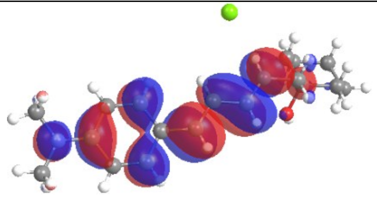
S1-HCl 374.3 nm; f = 1.178; 84 – 88 w = 1.0	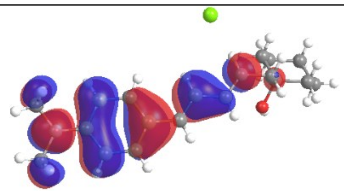	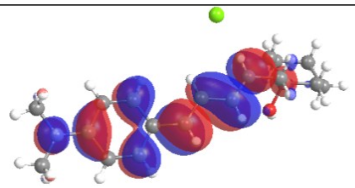

Figure S2. Natural transition orbitals for **S1** and [HCl(**S1**)] computed at PBE0/6-31+G(d,p)/IEF-PCM-Water.